ARTICLE   OPEN

Check for updates

Infinite critical boson non-Fermi liquid

Xiao-Tian Zhang [1,2] and Gang Chen [1,2✉]

We study a distinct type of non-Fermi liquid where there exists an infinite number of critical bosonic modes instead of finite number of bosonic modes for the conventional ones. We consider itinerant magnets with both conduction electrons and fluctuating magnetic moments in three dimensions. With Dzyaloshinskii–Moriya interaction, the moments fluctuate near a boson surface in the reciprocal space at low energies when the system approaches an ordering transition. The infinite number of critical modes on the boson surface strongly scatter the gapless electrons on the Fermi surface and convert the metallic sector into a non-Fermi liquid. We explain the physical properties of this non-Fermi liquid. On the ordered side, a conventional non-Fermi liquid emerges due to the scattering by the gapless Goldstone mode from the spontaneous breaking of the global rotational symmetry. We discuss the general structure of the phase diagram in the vicinity of the quantum phase transition and clarify various crossover behaviors.

INTRODUCTION

Landau Fermi liquid theory is the major milestone of modern condensed matter physics, and illustrates the triumph of physical intuition[1]. The short-range repulsive interaction between the fermions was argued to be irrelevant as one approaches the low energy towards the Fermi surface. The singular long-range interactions, however, are not well coped in the framework of Fermi liquid theory and signifies the possibility of non-Fermi liquid (NFL) metals[2,3]. These singular interactions can come from (partially screened) long-range Coulomb interaction, the fluctuations of the gapless bosonic modes at the criticality, the Goldstone boson from the continuous symmetry breaking[4], and the U(1) gauge boson[5,6]. The established theories describing NFL metals, particularly the experimentally relevant ones, are known as Hertz–Millis–Moriya theory[3,7–10]. This theory involves the coupling between gapless fermions near the Fermi surface and the critical bosons. If the number of the gapless fermions is finite such as Dirac fermion, Weyl fermion and the quadratic band touching, a controlled calculation with the perturbative renormalization group can be performed. In contrast, when the fermion sector is a Fermi surface, the physics become complex and this topic is under an active investigation in recent years.

So far there are two types of Fermi surface criticality associated NFLs[5]. The first involves an ordering at a finite wavevector, e.g., an antiferromagnetic (AFM) order[11–15] or spin density wave[16]. The ordering wavevector connects a few "hotspots" on the Fermi surface, and the theoretical analysis focuses on the coupling between the hotspot fermions and the critical bosons. The second involves the critical bosons at the zero wavevector. This captures, for instance, the Ising-nematic criticality[17–21], spinon-gauge coupling in the spinon Fermi surface U(1) spin liquid[6], ferromagnetic (FM) criticality[22,23]. It was observed that the bosons that are tangential to the Fermi surface scatter the fermions strongly at low energies. Thus, the theoretical analysis of this Ising-nematic criticality is further reduced to the so-called patch theory where the tangential critical boson scatters the fermions from one patch or two patches. Various analytic techniques were developed. The early random phase approximation type of large-N expansion was questioned as this scheme of taming quantum fluctuations and

organizing the Feynman diagrams misses the contribution from the processes involving the fermions on the Fermi surface[6,20,24–26]. The remedy was made by the double expansion that combines the large-N expansion and the ϵ-expansion[27,28]. Another remedy introduces the dimensional and co-dimensional regularization to the Fermi surface, and develops a systematic framework to regulate the quantum fluctuations[14,21,29–31]. It is hoped that the physical cases are located in the regimes where these development can be applied. Inspired by these developments, we turn our attention to another type of Fermi surface criticality and NFL. Compared to the efforts in the literature, here we are more inclined to exploring the mechanism and phenomenology of the NFLs.

In this paper, we study the system with the Fermi surface coupled to the critical bosons on a continuously degenerate manifold, i.e., a boson surface in three-dimensional space(3D) as shown in Fig. 1. The critical phase of bosons in one dimension is the Luttinger liquid[32]. Focusing on the stability of such highly degenerate critical phase in higher dimensions has been investigated in the context of Bose metal[33–38], and recent studies declared that weakly interacting dilute bosonic systems with continuously degenerate minima in the low-energy bosonic excitations are stable in $d = 2, 3$ and thereby pointed to the concept of Bose Luttinger liquid[39,40]. Experimentally, the relevance of critical boson surface has been implied by the neutron scattering in MnSi[41,42] where a nearly uniform intensity is measured on a sphere. Motivated by these developments, the investigation on the critical boson surface has received some attentions[43–45]. Here, we are neither dealing with nor relying on the stable phase of critical boson surfaces, instead we aim to improve our understanding of the critical boson surface-induced quantum criticality and its impact when it is coupled with gapless fermions.

We consider the 3D itinerant magnets that comprise two distinct types of degrees of freedom: (i) conduction electrons, (ii) local magnetic moments. In the absence of inversion symmetry, there exists a Dzyaloshinskii–Moriya interaction between the local moments that is responsible for the generation of infinite critical bosons on a spherical surface at the phase transition. The critical boson surface is coupled to the fermions on the Fermi surface at low energies through a Yukawa-type interaction. Microscopically,

[1]Department of Physics and HKU-UCAS Joint Institute for Theoretical and Computational Physics at Hong Kong, The University of Hong Kong, Pokfulam Road, Hong Kong SAR, China. [2]The University of Hong Kong Shenzhen Institute of Research and Innovation, 518057 Shenzhen, Guangdong Province, China. ✉email: gangchen@hku.hk
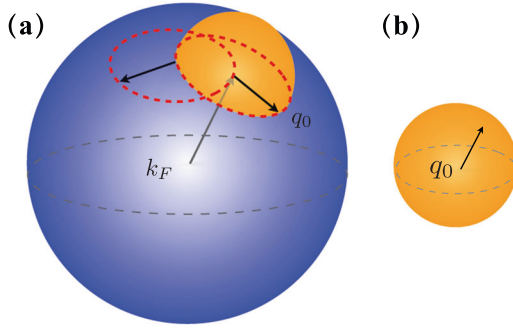
Fig. 1 The coupling between Fermi surface and critical boson surface. a The blue sphere is the Fermi surface of the conduction electrons. The orange surface represents the critical boson surface. k_F is the Fermi momentum, and q_0 is the radius of the boson surface. The Yukawa coupling connects fermions with a ring of fermion modes on the Fermi surface. **b** The critical boson sphere.

this Yukawa coupling arises from the Hund's or Kondo-like coupling between the conduction electron and the local moments. As illustrated in Fig. 1a, each fermion is coupled to a ring of fermions on the Fermi surface, and the fermions on this ring are further coupled to many other rings of fermions. Thus, infinite number of gapless fermions are scattered by the infinite number of critical bosons, which makes the whole Fermi surface critical. This fermion–boson-coupled model is fundamentally different from the AFM criticality or the Ising-nematic criticality where only a finite number of critical bosons are involved. Thus, neither the hotspot treatment for the AFM criticality nor the conventional patch theory is applicable. We establish the basic properties and the global phase diagram of the system, and adopt the self-consistent renormalization theory[10] to address the properties near the criticality. We show that, due to the novel type of fermion–boson coupling, the system becomes a NFL metal with distinct power law behaviors in the vicinity of the transition. We analyze the fermion and the boson properties as well as the related crossovers at the criticality and in the ordered regime.

RESULTS

Model

The full model for the itinerant magnets contains three parts, the conducting electrons, the local moments, and the coupling between them, which is then described by a fermion–boson-coupled Lagrangian

$$\mathcal{L}[f^\dagger, f; \overrightarrow{\phi}] = \sum_{l,a} f_{la}^\dagger (\partial_\tau - \mu) f_{la} - \sum_{ll',a} t_{ll'} f_{la}^\dagger f_{l'a}$$
$$+ g \sum_{l,\alpha\beta} f_{la}^\dagger \overrightarrow{\sigma}_{\alpha\beta} f_{l\beta} \cdot \overrightarrow{\phi}_l + \mathcal{L}_B[\overrightarrow{\phi}]. \quad (1)$$

The first line of Eq. (1) dictates an electron model where $f^\dagger(f)$ is the fermion creation (annihilation) operator. The itinerant electrons hop on a 3D lattice denoted by the site index l. The electron spin couples to a magnetic moment field $\overrightarrow{\phi}_l$ with a Kondo-like Yukawa coupling. Here, the bosonic field $\overrightarrow{\phi}_l$ is a three-component vector defined on site l, $\overrightarrow{\sigma}_{\alpha\beta}$ is the Pauli matrix vector with α, β being the spin indices. The magnetic fluctuation near the phase transition admits a standard Ginzburg–Landau expansion up to $\mathcal{O}(\phi^4)$ with

$$\mathcal{L}_B[\overrightarrow{\phi}] = \sum_l \frac{1}{2} \overrightarrow{\phi}_l \cdot (r - J\nabla^2) \overrightarrow{\phi}_l + \frac{u}{4} \left(\overrightarrow{\phi}_l^2\right)^2 + \frac{D}{2} \overrightarrow{\phi}_l \cdot (\nabla \times \overrightarrow{\phi}_l), \quad (2)$$

The first two terms of $\mathcal{L}_B[\overrightarrow{\phi}]$ represent a standard ϕ^4-theory with an order parameter $\overrightarrow{\phi}$ for the magnetic moment and r is the boson
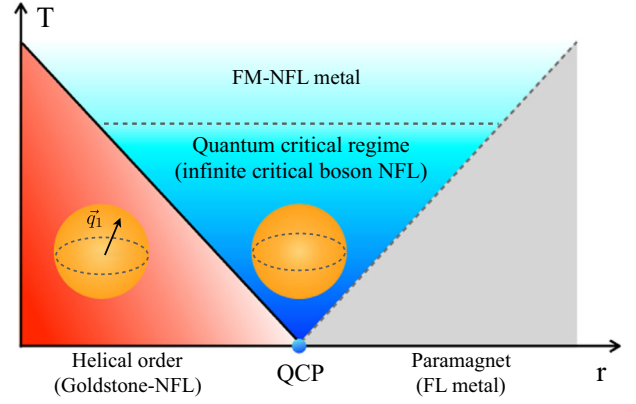

Fig. 2 The global phase diagram. The left corner is a helimagnet and a Goldstone-NFL where the NFL is induced by the gapless Goldstone boson. The right corner is a paramagnet and Fermi liquid metal. The central region is the quantum critical regime where a distinct NFL with infinite critical bosons on the boson surface is realized. As the temperature rises to the point where the thermal fluctuation submerges the boson surface, the system experiences a crossover to a FM criticality-like NFL behavior. The solid (dashed) line refers to the phase transition (thermal crossover).
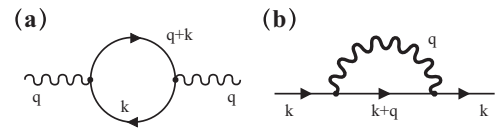

Fig. 3 Renormalized bubble diagrams. a The fermion bubble induced boson dynamics. **b** The renormalized fermion propagator from the renormalized boson correlator. The light and bold curly line represent the bare and renormalized boson correlators, respectively.

mass. The last term is an anti-symmetric Dzyaloshinskii–Moriya (DM) interaction, which fundamentally alters the critical phenomenon and leads to a rich phase diagram in Fig. 2.

To tackle with the bosonic fluctuation, a saddle point solution of $\overrightarrow{\phi}$ is required, on top of which the lowest order expansion counts for the fluctuations. As shown in Fig. 3, we follow the Hertz approach by integrating out the gapless fermions. This gives rise to the Landau damping that dominates the low-energy boson dynamics. The effective action for the bosonic sector is written as,

$$\mathcal{S}_B = \frac{1}{2} \sum_{\mathbf{q}, i\omega_l} \Pi_{\mu\nu}(\mathbf{q}, i\omega_l) \phi_\mu(\mathbf{q}, i\omega_l) \phi_\nu(-\mathbf{q}, -i\omega_l)$$
$$+ \frac{u}{4} \int d\tau \int d^3\mathbf{r} \left[\overrightarrow{\phi}^2(\mathbf{r}, \tau)\right]^2, \quad (3)$$

where μ, ν, λ label the vector components of $\overrightarrow{\phi}$, and we have converted the 3D lattice index to a continuous, real space coordinate $\mathbf{r}$. The fermionic bubble is illustrated in Fig. 3 and the renormalized boson polarization takes the form

$$\Pi_{\mu\nu}(\mathbf{q}, i\omega_l) = f(q, i\omega_l)\delta_{\mu\nu} - iD\epsilon_{\mu\nu\lambda} q_\lambda,$$
$$f(q, i\omega_l) = r + Jq^2 + \frac{|\omega_l|}{\Gamma_q}, \quad (4)$$

where $\omega_l = 2\pi l\beta^{-1} (l \in \mathbb{Z})$ is the Matsubara frequency for the bosons, and the $|\omega_l|/\Gamma_q$ is the Landau damping term. In general, the function Γ_q takes a form $\Gamma_q = \Gamma q$ with $q = |\mathbf{q}|$.

Critical boson surface

The DM interaction complicates the low-energy theories by introducing the vector index into the bosonic sector. The dispersion of the bosonic modes is modified compared to the $D = 0$ case. Diagonalizing the bare quadratic bosonic part at $\omega_l = 0$, we obtain three branches of bosonic modes with

dispersions given by

$$E_n(q) = r + Jq^2 + nDq, \quad n = -1, 0, +1. \tag{5}$$

The lowest branch $E_{-1}(q)$ is of particular interest, which reaches its minima on a spherical surface in the momentum space $q = q_0 \equiv D/(2J)$. Approaching the criticality at $r_c = D^2/(4J)$, the lowest mode $E_{-1}(q)$ becomes gapless at the surface $q = q_0$. Thus, the boson modes on the entire sphere $q = q_0$ become critical simultaneously, which is then dubbed "critical boson surface". The finite radius of the sphere is guaranteed by the DM interaction. The function $\Gamma_q \approx \Gamma q_0$, and Γ is a constant due to the finite density of states on the Fermi surface.

For a pure classical boson system, the large phase space provided by the critical boson surface always results in a fluctuation-driven first-order transition[46]. The low-energy dynamics of the fermion-boson coupled system is not determined by the critical boson surface alone; rather the boson receives renormalization from the particle-hole excitation around Fermi surface. A previous work by Schmalian and Turlakov[47] shed light on the nature of the quantum phase transition in the presence of the critical boson surface for a fermion-boson coupled system. The effective low-energy theory of the critical bosons are obtained by projecting onto the $n = -1$ mode in Eq. (5), which turns out to be a ϕ^4-theory with multiple quartic interaction constants. In certain parameter regimes, the transition can be a second-order transition in the university class $d = 3, z = 2$, and a mean-field theory of this second-order transition has been developed[48]. In the following, we regard that our system undergoes a second-order quantum transition and treat the critical fluctuation around the quantum critical point perturbatively. This physical scenario is realized within a crossover regime $\xi_{Gi} \gg \xi \gg \xi_{DM}$[47,49]. Here $\xi_{DM} \sim q_0^{-1}$ is the length scale of DM interaction. When the correlation length $\xi \gg \xi_{DM}$, the fluctuation of the bosons is dominated by the critical boson surface. The opposite limit $\xi \ll \xi_{DM}$ dictates a high-temperature regime in the phase diagram of Fig. 2. In addition, we regard that the fluctuations are weakly interacting according to the Ginzburg criteria $\xi \gg \xi_{Gi}$, and will carry out the self-consistent renormalization study next.

Self-consistent renormalization theory

Although the patch and the hotspot theories are inadequate for our fermion–boson-coupled model, a phenomenological technique, dubbed the self-consistent renormalization (SCR) theory[10,50], captures the key features of the fermion–boson coupling and provides the evidence for the behaviors near the criticality. The spirit of the SCR approach is to find the most appropriate quadratic action that encodes the effective renormalized non-linear interactions. This approach works well with $d = 3, z = 2$ and quantitatively produces the experimental results in many itinerant magnets of various dimensions[2] and works for continuous and nearly continuous transitions[8,9]. We here make an attempt to implement the SCR calculation for our fermion–boson-coupled model and hope to gain some understanding about the physical properties of the model. Moreover, since the SCR approach has never been applied to itinerant magnets with degenerate low-energy critical modes, our attempt would add one physical example to the SCR theory.

To search for the best action in the SCR approach, one relies on Feynman's variational method to optimize the free energy. Following the procedure by Moriya[10], we consider a trial quadratic action with the following form

$$\tilde{S}_B[\tilde{r}] = \frac{1}{2} \sum_{\mathbf{q}, i\omega_l} \left[\left(\tilde{r} + Jq^2 + \frac{|\omega_l|}{\Gamma_q} \right) \delta_{\mu\nu} - iD\epsilon_{\mu\nu\lambda}q_\lambda \right] \\ \times \phi_\mu(\mathbf{q}, i\omega_l)\phi_\nu(-\mathbf{q}, -i\omega_l), \tag{6}$$

where we replace r with a variational parameter $\tilde{r}$ that is to be determined. The boson correlator is given as a hermitian matrix

$M_{\mu\nu}$ (see Supplementary Note 6 for derivations),

$$\langle \phi_\mu(\mathbf{q}, i\omega_l)\phi_\nu(\mathbf{q}', i\omega_{l'}) \rangle_{\tilde{S}_B} \simeq M_{\mu\nu}(\mathbf{q}, i\omega_l)\delta_{\mathbf{q}, -\mathbf{q}'}\delta_{i\omega_l, -i\omega_{l'}} \tag{7}$$

where $\langle \cdots \rangle_{\tilde{S}_B}$ refers to the statistical average against $\tilde{S}_B$. This correlation conceives the information of the critical boson surface, and serves as a key ingredient for the mechanism of the proposed NFL that can be detected by the neutron scattering experiment. At the criticality, the powder-averaged neutron scattering spectrum is given as $\text{Tr}\, M(\mathbf{q}, \omega) \sim (\omega/\Gamma_{q_0})/[J^2(q - q_0)^4 + (\omega/\Gamma_{q_0})^2]$. Around the critical boson surface $|\mathbf{q}| = q_0$, the spectrum displays a divergent behavior. In the real space, the boson surface momentum q_0 provides a characteristic length scale $1/q_0$, which endows the correlation function with a spatial modulation in all directions, and the correlator from the elastic neutron scattering is given by an envelop function on top of the usual power law decaying in the long-distance limit as $\sum_\mu \langle \phi_\mu(\mathbf{r})\phi_\mu(0) \rangle_{\tilde{S}_B} \sim \sin(q_0|\mathbf{r}|)/|\mathbf{r}|^2$.

The variational free energy for the bosonic sector is

$$F(\tilde{r}) \equiv \tilde{F}(\tilde{r}) + \frac{1}{\beta} \langle S_B - \tilde{S}_B \rangle_{\tilde{S}_B}$$

$$= \tilde{F}(\tilde{r}) + \frac{1}{2\beta}(r - \tilde{r})\left[\text{Tr} \sum_{\mathbf{q}, i\omega_l} M(\mathbf{q}, i\omega_l) \right] + \frac{u}{4\beta^2 V}$$

$$\times \left\{ \left[\text{Tr} \sum_{\mathbf{q}, i\omega_l} M(\mathbf{q}, i\omega_l) \right]^2 + 2\,\text{Tr}\left[\sum_{\mathbf{q}, i\omega_l} M(\mathbf{q}, i\omega_l) \right]^2 \right\}, \tag{8}$$

where $\tilde{F}(\tilde{r})$ is the free energy corresponding to the trial quadratic action $\tilde{S}_B$, and V is the system volume. The variational parameter $\tilde{r}$ is determined from the saddle point equation $\partial_{\tilde{r}}F(\tilde{r}) = 0$. After the cumbersome calculation detailed in Supplementary Note 1, the optimization procedure results in the following self-consistent equation for the parameter $\tilde{r}$,

$$\tilde{r} - r = \frac{uc}{\beta V} \sum_{n = \pm 1, 0} \sum_{\mathbf{q}, i\omega_l} \frac{1}{|\omega_l|/\Gamma_q + \mathcal{E}_n(q)}, \tag{9}$$

where $\mathcal{E}_n(q) = E_n(q)|_{r \to \tilde{r}}$ and c is a constant prefactor. We further set $\delta \equiv \tilde{r} - r_c$ and $\delta_0 \equiv r - r_c$. Here, δ measures the distance from the quantum critical point $\delta_c = 0$ and is related to the correlation length $\xi(T)$ that is expected to diverge at the criticality at low temperatures with $\delta(T) = \xi^{-2}(T)$. From the above self-consistent equation, we find that the quantum fluctuation at finite temperatures is encoded in the function $\delta(T)$ that scales as (see Supplementary Note 2 for derivations)

$$\delta(T) \sim T^a, \quad a = \frac{4}{5}. \tag{10}$$

It is illuminating to compare with the behaviors for the 3D FM (AFM) criticality where the dynamic exponent $z = 3(z = 2)$ and the SCR calculation yields $a = 4/3(a = 3/2)$. In fact, the same exponents were obtained from a simple scaling counting using Millis's renormalization $a = (d + z - 2)/z^2$. For both FM and AFM criticality, $a > 1$. In contrast, $a < 1$ in Eq. (10) indicates much stronger fluctuations due to the extensive phase space provided by the critical boson surface.

NFL behavior from critical boson surface

Unlike the FM or AFM criticalities where the low-energy fluctuations are at discrete momenta, the low-energy fluctuations near a finite boson surface strongly scatter the itinerant electrons and reduce the lifetime of electron quasiparticles. We use the renormalized boson correlator and the Feymann diagram in Fig. 3 to calculate the self-energy of the conduction electron,

$$\Sigma(\mathbf{k}, i\epsilon_n) \simeq \frac{g^2}{\beta V} \sum_{\mathbf{q}, i\omega_l} G_0(\mathbf{k} + \mathbf{q}, i\epsilon_n + i\omega_l)\,\text{Tr}\,[M(\mathbf{q}, i\omega_l)], \tag{11}$$

where $\epsilon_n \equiv (2n+1)\pi/\beta (n \in \mathbb{Z})$ is the fermion Matsubara frequency, and $G_0(\mathbf{k}, i\epsilon_n) = (i\epsilon_n - \xi_\mathbf{k})^{-1}$ is a bare Green's function of the electrons with a dispersion $\xi_\mathbf{k} \equiv \mathbf{k}^2/(2m) - \epsilon_F$. By performing an analytic continuation $i\epsilon_n \to \omega + i\eta$, we obtain the T-dependence for the retarded self-energy in the static limit $\omega = 0$ with $|\mathbf{k}| = k_F$ located on the Fermi surface (see Supplementary Note 4 for derivations),

$$\text{Im}\Sigma^R(\mathbf{k}, \omega = 0; T) \sim T^3 \delta^{-2} \sim T^{3-2a}. \tag{12}$$

We note the T-dependence here has multiple sources that might render a simple scaling $\sim \omega/T$ inappropriate. We can see this by evaluating the ω-dependence of the self-energy in the zero temperature limit is evaluated in Supplementary Note 5, which yields $\text{Im}\Sigma^R(\mathbf{k}, \omega; T = 0) \sim \sqrt{\omega}$. This result is consistent with literature[47].

The imaginary part of the self-energy in Eq. (12) determines the scattering rate for the forward scattering process provided the exchanged boson momentum is small $q_0 \ll k_F$. The electronic resistivity (or the inverse transport lifetime) is obtained from the scattering rate by multiplying an angular factor $(1 - \cos\theta)$, where $\theta \simeq q_0/k_F \ll 1$ is the small forward scattering angle. The narrow scattering angle suppress the resistivity by $\sim (q_0/k_F)^2$, and more importantly, the T-dependence is inherited from Eq. (12) as,

$$\rho(T) \sim \frac{q_0^2}{2k_F^2} \text{Im}\Sigma^R(\mathbf{k}, \omega = 0; T) \sim T^{7/5}. \tag{13}$$

This peculiar power law T-dependence indicates a distinct NFL behavior owing to the scattering of the electrons by the extensive critical fluctuations on the boson surface. The accuracy of this study is limited by the phenomenological method we used, namely, we only considered small-angle forward scattering. Whereas the large-angle scattering processes enabled by multiple scatterings on the Fermi surface are neglected. Moreover, the SCR method represents a way to bypass the significant challenge that it is extremely difficult to cook up a low-energy effective theory.

Crossover to FM-NFL at high-T

We have discussed the NFL behavior arised from the strong fluctuations near the boson surface at low-T which is quoted as an infinite critical boson NFL. When the temperature is further increased to be larger than a characteristic energy associated with the boson sphere radius q_0, i.e., $T \gg \Gamma_{q_0}$, the fluctuation is no longer dominated by the boson modes near the critical surface. In fact, the structure of the critical boson surface is no longer discernible at high temperatures. The boson sphere can be regarded as a point object in the reciprocal space, resembling the case of the FM criticality. In this high-temperature regime above the criticality, the temperature dependence of the variational parameter crossovers to scale as $\delta(T) \sim T^{4/3}$, which coincides with the case of the NFL from the FM fluctuations in 3D. The calculation is shown in Supplementary Note 3. Thus, the system undergoes a crossover between two distinct types of NFLs (see Fig. 2), and the crossover temperature can be approximately set by the difference of the boson energies at the center and at the surface of the boson sphere,

$$T_c \sim E_{-1}(q = 0) - E_{-1}(q_0) \sim \mathcal{O}\left(\frac{D^2}{4J}\right). \tag{14}$$

NFL in the helimagnetic ordered phase

When $r < r_c$, the system develops a magnetic order by spontaneously selecting the ordering wavevector from the degenerate boson surface [see Supplementary Note 7 for more discussions]. In the left corner of the phase diagram in Fig. 2, a helical order with an ordering wavevector at $\mathbf{q}_1 = q_0\hat{n}$ is picked up where $\hat{n}$ is the

propagating direction of the helimagnet. The original model in Eq. (1) is invariant under a combined rotation with respect to the real space and the internal space of the magnetic orders. The helimagnet spontaneously breaks this continuous symmetry and thus generates gapless Goldstone modes. In the helimagnetic phase, a small fluctuation above the helical order parameter couples to the itinerant electrons with

$$\sim g \int d^3\mathbf{r} f_\alpha^\dagger(\mathbf{r}) \overrightarrow{\sigma}_{\alpha\beta} f_\beta(\mathbf{r}) \cdot \delta\overrightarrow{\phi}(\mathbf{r}), \tag{15}$$

where $\delta\overrightarrow{\phi}(\mathbf{r}) = \phi_0[-\varphi(\mathbf{r})\sin q_0 z, \varphi(\mathbf{r})\cos q_0 z, \theta(\mathbf{r})]$ with $\theta(\mathbf{r})$ and $\varphi(\mathbf{r})$ describing the polar and the azimuthal phase fluctuations against the helical order $\langle\overrightarrow{\phi}(\mathbf{r})\rangle = \phi_0[\cos(q_0 z)\hat{x} + \sin(q_0 z)\hat{y}]$ with $\hat{n} = \hat{z}$. These phase fluctuations give rise to gapless Goldstone modes[51]. The Yukawa coupling, g, remains finite in the low-energy limit. This is due to the fact that the generator for the continuous symmetry involves the orbital angular momentum and thus does not commute with the translation operator, i.e., the total momentum. Applying the general criteria in ref. [4], we see that the Goldstone mode converts the fermion sector into a NFL which is dubbed "Goldstone-NFL". The NFL behavior in the helimagnetic phase, e.g., the electronic resistivity, has been discussed[52,53].

DISCUSSION

In summary, we have studied a distinct type of NFL in the 3D itinerant magnets that are not captured by the conventional patch and hotspot theories. The infinite critical boson modes on the boson sphere connect all momentum points on the Fermi surface for the itinerant electrons, leading to unconventional consequences for both local moments and itinerant electrons. The SCR approach adopted in our study is a phenomenological method that has been proven to be successful in explaining the FM and the AFM fermion criticalities[10]. For the continuously degenerate boson surface criticality, the SCR approach incorporates the large scattering phase space between fermions and bosons where the renormalized fermionic and bosonic correlations are taken into consideration sequentially.

On the more experimental side, several further investigations with material-based simulations can be expected. In reality, the boson sector would experience a cubic anisotropy in the interaction that would favor the wavevectors along either 001 or 111 directions and thus lift the degeneracy of the boson surface. This cubic anisotropy could set another crossover energy scale for the problem. The effect of external fields such as the pressure and magnetic field is anticipated due to its relevance to the experiments on MnSi[41,42]. An anomalous NFL transport behavior is observed in a widespread region of the phase diagram spanned by pressure and magnetic field. The experimental relevance of the infinite critical boson NFL to physical systems like MnSi may be addressed in a specific study with a more realistic consideration. In general, the role of a finite uniform magnetic field is two-folded. First, it leads to the procession of the spin order parameter, which competes with the Landau damping dynamics caused by the fermion. Second, this external field introduces anisotropy for the quantum critical points, which may effectively reduce the fluctuating dimension of the boson sector. Intuitively, the 2D counterpart of the present problem can be readily considered where a Fermi circle is coupled to a 1D critical boson contour. This critical boson contour can appear, for instance, on the interface of magnetic heterostructure[54] or in 2D-frustrated magnets[55]. Particular interest lies in the situation where the radius of the boson contour can be commensurate or incommensurate to the Fermi circle. For the commensurate cases, only finite Fermi points are connected by the boson contour. The crossover/transition to incommensurate cases bridges the infinite critical boson NFL with the conventional one described by the hotspot theory. Moreover, one can consider the fermion–boson-coupled system in mixed

dimensions, namely, the dimension of the Fermi surface is incompatible with critical boson modes. One intuitive example can be found in the 3D fractional quantum Hall system[56]. Soft gauge bosons in 3D bulk can couple with the chiral Fermi level of the partons on the 2D surface[56], which may trigger a NFL instability on the surface. Beyond the scope of condensed matter physics, this general framework may apply to the meson–neutron coupling in neutron stars where the meson condensation forms a degenerate boson surface[57].

DATA AVAILABILITY

The possible data that support the findings of this study are available from the corresponding author (G.C.) upon request.

REFERENCES

1. Landau, L. D., Lifshitz, E. M. & Pitaevskii, L. *Statistical Physics: Theory of the Condensed State* (Butterworth-Heinemann, 1980).
2. Löhneysen, H. V., Rosch, A., Vojta, M. & Wölfle, P. Fermi-liquid instabilities at magnetic quantum phase transitions. *Rev. Mod. Phys.* **79**, 1015–1075 (2007).
3. Hertz, J. A. Quantum critical phenomena. *Phys. Rev. B* **14**, 1165–1184 (1976).
4. Watanabe, H. & Vishwanath, A. Criterion for stability of Goldstone modes and Fermi liquid behavior in a metal with broken symmetry. *Proc. Natl Acad. Sci. USA* **111**, 16314–16318 (2014).
5. Lee, S.-S. Recent developments in non-Fermi liquid theory. *Annu. Rev. Condens. Matter Phys.* **9**, 227–244 (2018).
6. Lee, S.-S. Low-energy effective theory of Fermi surface coupled with U(1) gauge field in $2 + 1$ dimensions. *Phys. Rev. B* **80**, 165102 (2009).
7. Millis, A. J. Effect of a nonzero temperature on quantum critical points in itinerant fermion systems. *Phys. Rev. B* **48**, 7183–7196 (1993).
8. Moriya, T. & Kawabata, A. Effect of spin fluctuations on itinerant electron ferromagnetism. *J. Phys. Soc. Jpn.* **34**, 639–651 (1973).
9. Moriya, T. & Kawabata, A. Effect of spin fluctuations on itinerant electron ferromagnetism. II. *J. Phys. Soc. Jpn.* **35**, 669–676 (1973).
10. Moriya, T. *Spin Fluctuations in Itinerant Electron Magnetism* (Springer Science & Business Media, 2012).
11. Abanov, A. & Chubukov, A. V. Spin-fermion model near the quantum critical point: one-loop renormalization group results. *Phys. Rev. Lett.* **84**, 5608–5611 (2000).
12. Abanov, A. & Chubukov, A. Anomalous scaling at the quantum critical point in itinerant antiferromagnets. *Phys. Rev. Lett.* **93**, 255702 (2004).
13. Abrahams, E. & Wölfle, P. Critical quasiparticle theory applied to heavy fermion metals near an antiferromagnetic quantum phase transition. *Proc. Natl Acad. Sci. USA* **109**, 3238–3242 (2012).
14. Sur, S. & Lee, S.-S. Quasilocal strange metal. *Phys. Rev. B* **91**, 125136 (2015).
15. Schlief, A., Lunts, P. & Lee, S.-S. Exact critical exponents for the antiferromagnetic quantum critical metal in two dimensions. *Phys. Rev. X* **7**, 021010 (2017).
16. Metlitski, M. A. & Sachdev, S. Quantum phase transitions of metals in two spatial dimensions. II. Spin density wave order. *Phys. Rev. B* **82**, 075128 (2010).
17. Oganesyan, V., Kivelson, S. A. & Fradkin, E. Quantum theory of a nematic Fermi fluid. *Phys. Rev. B* **64**, 195109 (2001).
18. Metzner, W., Rohe, D. & Andergassen, S. Soft Fermi surfaces and breakdown of Fermi-liquid behavior. *Phys. Rev. Lett.* **91**, 066402 (2003).
19. Lawler, M. J. & Fradkin, E. Local quantum criticality at the nematic quantum phase transition. *Phys. Rev. B* **75**, 033304 (2007).
20. Metlitski, M. A. & Sachdev, S. Quantum phase transitions of metals in two spatial dimensions. I. Ising-nematic order. *Phys. Rev. B* **82**, 075127 (2010).
21. Dalidovich, D. & Lee, S.-S. Perturbative non-Fermi liquids from dimensional regularization. *Phys. Rev. B* **88**, 245106 (2013).
22. Rech, J., Pépin, C. & Chubukov, A. V. Quantum critical behavior in itinerant electron systems: Eliashberg theory and instability of a ferromagnetic quantum critical point. *Phys. Rev. B* **74**, 195126 (2006).
23. Chubukov, A. V. & Maslov, D. L. Spin conservation and Fermi liquid near a ferromagnetic quantum critical point. *Phys. Rev. Lett.* **103**, 216401 (2009).
24. Polchinski, J. Low-energy dynamics of the spinon-gauge system. *Nucl. Phys. B* **422**, 617–633 (1994).
25. Altshuler, B. L., Ioffe, L. B. & Millis, A. J. Low-energy properties of fermions with singular interactions. *Phys. Rev. B* **50**, 14048–14064 (1994).
26. Kim, Y. B., Lee, P. A. & Wen, X.-G. Quantum Boltzmann equation of composite fermions interacting with a gauge field. *Phys. Rev. B* **52**, 17275–17292 (1995).
27. Nayak, C. & Wilczek, F. Non-Fermi liquid fixed point in $2 + 1$ dimensions. *Nucl. Phys. B* **417**, 359–373 (1994).
28. Mross, D. F., McGreevy, J., Liu, H. & Senthil, T. Controlled expansion for certain non-Fermi-liquid metals. *Phys. Rev. B* **82**, 045121 (2010).
29. Chakravarty, S., Norton, R. E. & Syljuåsen, O. F. Transverse gauge interactions and the vanquished Fermi liquid. *Phys. Rev. Lett.* **74**, 1423–1426 (1995).
30. Senthil, T. & Shankar, R. Fermi surfaces in general codimension and a new controlled nontrivial fixed point. *Phys. Rev. Lett.* **102**, 046406 (2009).
31. Mandal, I. & Lee, S.-S. Ultraviolet/infrared mixing in non-Fermi liquids. *Phys. Rev. B* **92**, 035141 (2015).
32. Giamarchi, T. *Quantum Physics in One Dimension* (Clarendon Press, 2003).
33. Das, D. & Doniach, S. Existence of a Bose metal at $T = 0$. *Phys. Rev. B* **60**, 1261–1275 (1999).
34. Phillips, P. The elusive Bose metal. *Science* **302**, 243–247 (2003).
35. Paramekanti, A., Balents, L. & Fisher, M. P. A. Ring exchange, the exciton Bose liquid, and bosonization in two dimensions. *Phys. Rev. B* **66**, 054526 (2002).
36. Motrunich, O. I. & Fisher, M. P. A. *d*-wave correlated critical Bose liquids in two dimensions. *Phys. Rev. B* **75**, 235116 (2007).
37. Sheng, D. N., Motrunich, O. I. & Fisher, M. P. A. Spin Bose-metal phase in a spin-$\frac{1}{2}$ model with ring exchange on a two-leg triangular strip. *Phys. Rev. B* **79**, 205112 (2009).
38. Han, S. & Kim, Y. B. Non-Fermi liquid induced by Bose metal with protected subsystem symmetries. *Phys. Rev. B* **106**, L081106 (2022).
39. Sur, S. & Yang, K. Metallic state in bosonic systems with continuously degenerate dispersion minima. *Phys. Rev. B* **100**, 024519 (2019).
40. Lake, E., Senthil, T. & Vishwanath, A. Bose-Luttinger liquids. *Phys. Rev. B* **104**, 014517 (2021).
41. Pfleiderer, C., Julian, S. R. & Lonzarich, G. G. Non-Fermi-liquid nature of the normal state of itinerant-electron ferromagnets. *Nature* **414**, 427–430 (2001).
42. Pfleiderer, C. et al. Partial order in the non-Fermi-liquid phase of MnSi. *Nature* **427**, 227–231 (2004).
43. Lajer, M., Konik, R. M., Pisarski, R. D. & Tsvelik, A. M. When cold, dense quarks in $1 + 1$ and $3 + 1$ dimensions are not a Fermi liquid. *Phys. Rev. D.* **105**, 054035 (2022).
44. Hegg, A., Hou, J. & Ku, W. Geometric frustration produces long-sought Bose metal phase of quantum matter. *Proc. Natl Acad. Sci. USA* **118**, e2100545118 (2021).
45. Pan, Z. & Zhang, X.-T. Infinite critical boson induced non-Fermi liquid in $d = 3 − \epsilon$ dimensions. Preprint at https://arxiv.org/abs/2205.03818 (2022).
46. Brazovskii, S. A. Phase transition of an isotropic system to an inhomogeneous state. *Sov. Phys. JETP* **41**, 85–89 (1975).
47. Schmalian, J. & Turlakov, M. Quantum phase transitions of magnetic rotons. *Phys. Rev. Lett.* **93**, 036405 (2004).
48. Vojta, T. & Sknepnek, R. Quantum phase transition of itinerant helimagnets. *Phys. Rev. B* **64**, 052404 (2001).
49. Janoschek, M. et al. Fluctuation-induced first-order phase transition in Dzyaloshinskii-Moriya helimagnets. *Phys. Rev. B* **87**, 134407 (2013).
50. Nagaosa, N. *Quantum Field Theory in Strongly Correlated Electronic Systems* (Springer Science & Business Media, 1999).
51. Belitz, D., Kirkpatrick, T. R. & Rosch, A. Theory of Helimagnons in itinerant quantum systems. *Phys. Rev. B* **73**, 054431 (2006).
52. Kirkpatrick, T. R. & Belitz, D. Nonanalytic corrections to Fermi-liquid behavior in helimagnets. *Phys. Rev. B* **72**, 180402 (2005).
53. Belitz, D., Kirkpatrick, T. R. & Rosch, A. Theory of Helimagnons in itinerant quantum systems. II. nonanalytic corrections to Fermi-liquid behavior. *Phys. Rev. B* **74**, 024409 (2006).
54. Zhang, X.-T. & Chen, G. Infinite critical boson non-Fermi liquid on heterostructure interfaces. Preprint at https://arxiv.org/abs/2109.06594 (2021).
55. Liu, J. Q., Li, F.-Y., Chen, G. & Wang, Z. Featureless quantum paramagnet with frustrated criticality and competing spiral magnetism on spin-1 honeycomb lattice magnet. *Phys. Rev. Res.* **2**, 033260 (2020).
56. Levin, M. & Fisher, M. P. A. Gapless layered three-dimensional fractional quantum Hall states. *Phys. Rev. B* **79**, 235315 (2009).
57. Migdal, A., Saperstein, E., Troitsky, M. & Voskresensky, D. Pion degrees of freedom in nuclear matter. *Phys. Rep.* **192**, 179–437 (1990).

AUTHOR CONTRIBUTIONS

G.C. designed and supervised this project. X.T.Z. and G.C. performed the calculation and wrote the manuscript.

COMPETING INTERESTS

The authors declare no competing interests.

ADDITIONAL INFORMATION

Supplementary information The online version contains supplementary material available at https://doi.org/10.1038/s41535-023-00543-0.

Correspondence and requests for materials should be addressed to Gang Chen.

Reprints and permission information is available at http://www.nature.com/reprints